



Supernovae from the 8-10 M_{\odot} range: the first spectral models for the emission-line phase

A. Jerkstrand, T. Ertl, H.-T. Janka, and E. Müller

Max-Planck-Institute for Astrophysics, Karl-Schwarzschild - Str. 1, 85748 Garching, Germany
e-mail: anders@mpa-garching.mpg.de

Abstract. Stars in the $M_{ZAMS} = 8 - 10 M_{\odot}$ range are expected to account for about 1/3 of all core-collapse supernovae (SNe). Here we describe calculations of the first spectral models in the nebular phase ($t > 200$ d) for such SNe, and the diagnostic potential of these. Comparison of a 9 M_{\odot} SN model with SN 1997D suggests that the observational class of subluminescent Type IIP SNe is linked to the low-mass end of progenitors. We discuss potential diagnostics of electron capture supernovae from ^{58}Ni lines.

Key words. Stars: supernovae

1. Introduction

The threshold for stars to make core-collapse supernovae is believed to be about 8 M_{\odot} . Due to the steepness of the star formation initial mass function (IMF), almost 30% of all CCSNe are expected to occur in the 8-10 M_{\odot} range. Historically this range has not been extensively modelled up to and through the core-collapse point due to large uncertainties and numerical challenges in the late stellar evolution stages. Consequently, there has also been a lack of light curve and spectral models needed to interpret about every third core-collapse supernova observed.

One of few progenitor models was calculated by Nomoto (1984), who found from an 8.8 M_{\odot} progenitor an ONeMg core that began collapse due to electron captures. Modern explosion simulations of this progenitor have demonstrated a robust neutrino-driven explosion even in 1D, giving an explosion energy of about 0.1 Bethe (e.g. Kitaura et al., 2006). This

kind of explosion, termed “electron capture supernova (ECSN)” produces iron-group elements by α -rich freeze-out of neutrino-heated matter that cools off from NSE temperatures, and eject these together with the unburnt He and H layers.

At higher mass values, the star instead evolves to iron core formation (Woosley & Heger, 2015). It has recently been demonstrated that progenitors on the very low mass end have similar explosion dynamics as ECSNe (Wanajo et al., 2017). Thus, the low-mass end of CCSN progenitors explode robustly, whether by collapse of ONeMg or Fe cores, with predicted energies of about 0.1 Bethe.

The observational class of “subluminescent Type IIP SNe” (Turatto et al., 1998; Pastorello et al., 2004) is the prime candidate class for the observational counterparts of 8-10 M_{\odot} explosions. These transients have narrow lines, low inferred explosion energies, and small amounts of ^{56}Ni , just as expected from theory for 8-10

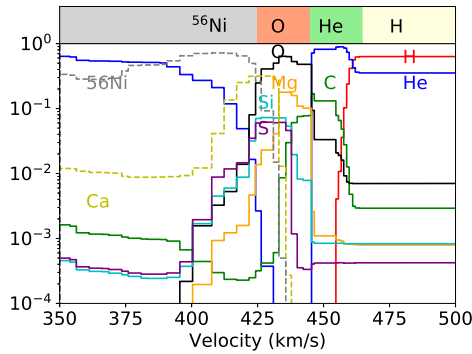


Fig. 1. Composition (mass fractions) of the explosion model.

M_{\odot} explosions. However, until now a lack of spectroscopic models for this mass range has prevented a detailed comparison. The goal of the current work is to make the first such model comparisons.

2. Method

Our starting point are neutrino-driven 1D explosion simulations of stars in the 9-11 M_{\odot} range (Sukhbold et al., 2016). These models were rerun to evolve to longer (homologous) times than in the original paper. In addition, the dynamic effects of radioactive decay were added. Figure 1 shows the composition in the 9 M_{\odot} explosion model versus velocity coordinate.

We then calculated physical conditions and spectra using the SUMO spectral synthesis code (Jerkstrand et al., 2011). SUMO computes the temperature and NLTE excitation/ionization solutions in each zone of the SN ejecta, taking a large number of physical processes into account. Specifically, the modelling consists of the following computational steps:

- (i) Emission, transport, and deposition of radioactive decay products (gamma-rays, X-rays, leptons).
- (ii) Determination of the distribution of non-thermal electrons created by the radioactivity.
- (iii) Thermal equilibrium in each compositional zone.

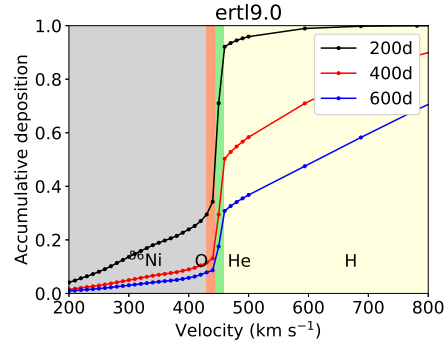


Fig. 2. Accumulative energy deposition from radioactive decay products. The zones are labelled with their most abundant element.

- (iv) NLTE ionization balance for the 20 most common elements.
- (v) NLTE excitation structure for about 50 atoms and ions.
- (vi) Radiative transfer through the ejecta.

The solutions are generally coupled to each other and global convergence is achieved by iteration.

3. Results

Figure 2 shows the accumulative gamma ray deposition in the 9 M_{\odot} model. The inner ^{56}Ni region traps 10-30% of the gamma rays (depending on epoch), the O/He shell 20-60%, and the H envelope a strongly time-varying 10% at 200d and 70% at 600d. This means that we expect emission lines from each layer of the SN, although the thin O shell absorbs relatively little energy and thus will not make very strong signatures.

Figure 3 shows the spectrum of the model at 400d, with the most prominent elements color coded. The model predicts distinct emission lines of H ($H\alpha$), He (7065 Å), C (8727 Å, 9850 Å), O (6300 Å, 7774 Å), Mg (4571 Å), and Ca (7300 Å, 8600 Å). Much of the quasi-continuum is made by Fe I. The use of realistic explosion physics, and consideration of β decays, mean that this prediction of line widths is to a large extent ab-initio.

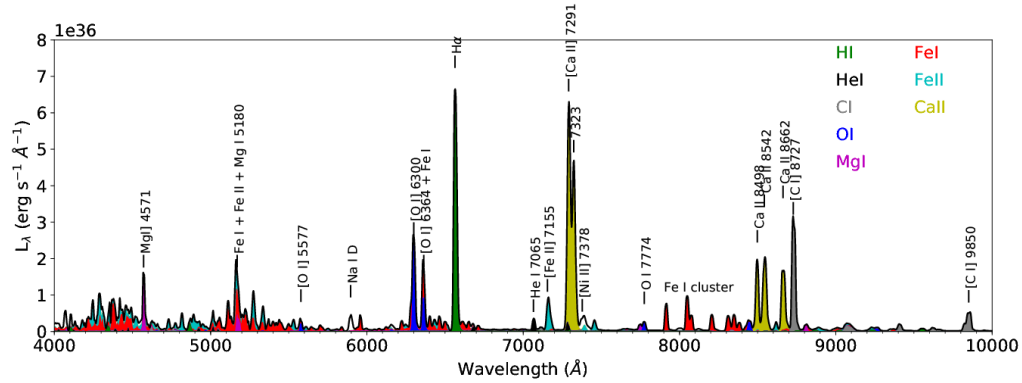


Fig. 3. Spectrum of 9 M_{\odot} explosion model at 400d.

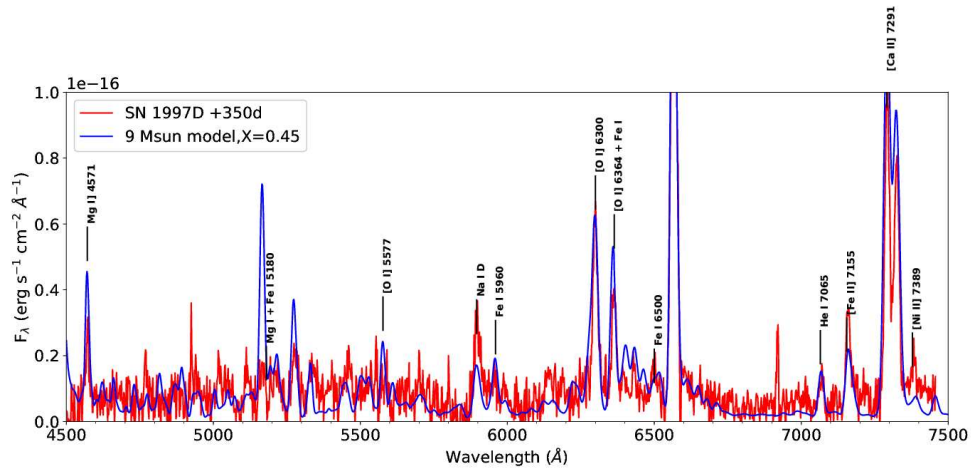


Fig. 4. Spectrum of 9 M_{\odot} explosion model at 400d, versus SN 1997D.

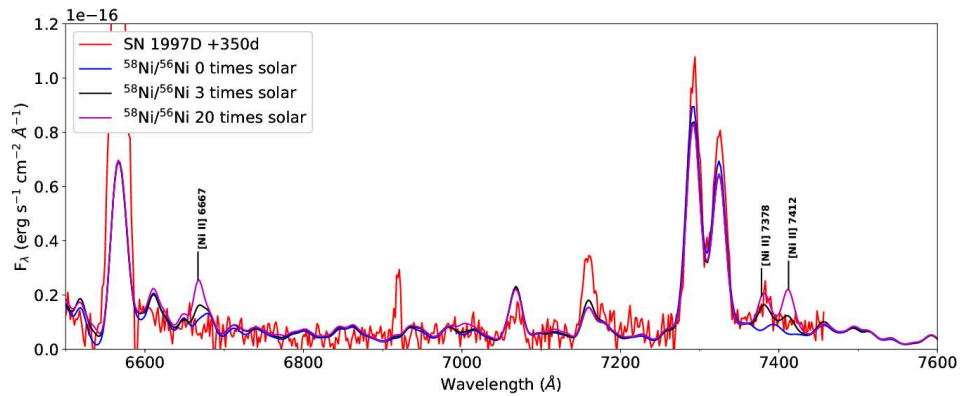


Fig. 5. Spectrum of 9 M_{\odot} explosion model at 400d, with varying amounts of ^{58}Ni added, versus SN 1997D.

3.1. Data comparison

In Fig. 4, the 9 M_{\odot} model is compared to SN 1997D (Benetti et al., 2001), the prototype for the “subluminous Type IIP class”, with low expansion velocities and low inferred ^{56}Ni mass. The model shows excellent agreement in both line profiles and luminosities for Mg I] 4571, Na I D, [O I] 6300, 6364, H α , He I 7065, [Fe II] 7065, [Ca II] 7291, 7323. Given the absence of any tunings of the model, apart from rescaling to the different ^{56}Ni mass in SN1997D (factor $X = 0.45$ lower than in our model), this agreement is quite remarkable and gives strong support for this model class.

The relative strength of [O I] 6300 and [O I] 6364 is of importance; this ratio depends on the oxygen density. As discussed by Chugai & Utrobin (2000), the deviation from the optically thick 1:1 ratio at quite early epochs in SN 1997D suggests small amounts of oxygen, and cannot easily be explained by massive progenitors, where a 1:1 ratio would be maintained for longer.

An interesting question is whether ECSNe can be spectroscopically distinguished from Fe CCSNe. One potential diagnostic is the very high Ni/Fe ratio of ~ 30 time solar predicted in ECSNe (Wanajo et al., 2009). The emission from nickel comes from ^{58}Ni at nebular times, as almost all ^{56}Ni has decayed. This isotope lacks in our explosion models. However, we performed a parameterized test by adding ^{58}Ni to have Ni/Fe ratios of zero, 3 and 20. Figure 5 compares these spectra with SN 1997D. At high Ni/Fe ratios, the model predicts quite strong [Ni II] 6667 and [Ni II] 7378, 7412. While [Ni II] 7378 can be fit with 30 times solar (but also lower), [Ni II] 6667 and [Ni II] 7412 are clearly too strong in such models.

4. Summary and conclusions

The first nebular-phase spectral models for SNe from stars with $M_{\text{ZAMS}} = 8 - 12 M_{\odot}$ have

been calculated by combined use of KEPLER stellar evolution models, P-HOTB explosion simulations, and SUMO spectral synthesis modelling. Despite the low amounts of nucleosynthesis, these models still show distinct signatures of e.g. He, Mg, and O. A model of a 9 M_{\odot} progenitor star exploded with 0.1 B exhibits close agreement with SN 1997D, suggesting that the class of subluminous IIP SNe is linked to 8-12 M_{\odot} progenitors. The lines from ^{58}Ni indicate that SN 1997D was a Fe CCSN, not an ECSN.

Acknowledgements. A. J. thank the conference organizers for a pleasant and stimulating meeting. A. J. acknowledges funding by the European Union’s Framework Programme for Research and Innovation Horizon 2020 under Marie Skłodowska-Curie grant agreement No 702538. This work has been supported by the Deutsche Forschungsgemeinschaft through the Excellence Cluster Universe EXC 153 and by the European Research Council through ERC-AdG No. 341157- COCO2CASA.

References

- Benetti, S., Turatto, M., Balberg, S., et al. 2001, MNRAS, 322, 361
- Chugai, N. N. & Utrobin, V. P. 2000, A&A, 354, 557
- Jerkstrand, A., Fransson, C., & Kozma, C. 2011, A&A, 530, A45
- Kitaura, F. S., Janka, H.-T., & Hillebrandt, W. 2006, A&A, 450, 345
- Nomoto, K. 1984, ApJ, 277, 791
- Pastorello, A., Zampieri, L., Turatto, M., et al. 2004, MNRAS, 347, 74
- Sukhbold, T., Ertl, T., Woosley, S. E., Brown, J. M., & Janka, H.-T. 2016, ApJ, 821, 38
- Turatto, M., Mazzali, P. A., Young, T. R., et al. 1998, ApJ, 498, L129
- Wanajo, S., et al. 2017, ArXiv:1701.06786
- Wanajo, S., et al. 2009, ApJ, 695, 208
- Woosley, S. E. & Heger, A. 2015, ApJ, 810, 34